INTERFACE TRACKING BASED EVALUATION OF BUBBLE GROWTH RATES IN HIGH PRESSURE POOL BOILING CONDITIONS

J. Murallidharan and G. Giustini
Department of Mechanical Engineering, Imperial College London
London SW7 2AZ, UK
j.murallidharan@imperial.ac.uk; g.giustini@imperial.ac.uk

Y. Sato and B. Ničeno
Nuclear Energy and Safety Research Department, Paul Scherrer Institute
Villigen, PSI 5232, Switzerland
yohei.sato@psi.ch; bojan.niceno@psi.ch

V. Badalassi and S.P. Walker
Department of Mechanical Engineering, Imperial College London
London SW7 2AZ, UK
v.badalassi@imperial.ac.uk; s.p.walker@imperial.ac.uk

ABSTRACT

Component-scale modeling of boiling is predominantly based on the Eulerian-Eulerian two-fluid approach. Within this framework, wall boiling is accounted for via the RPI model, and within this model, the nucleating bubble is characterized using three main parameters: departure diameter (D), nucleation site density (N) and departure frequency (f). Typically, the magnitudes of these three parameters are obtained from empirical correlations. However, in recent years, efforts have been directed towards mechanistic modeling of the boiling process. Of the three parameters mentioned above, the departure diameter (D) is the least affected by the intrinsic uncertainties of the nucleate boiling process. This feature, along with its prominence within the RPI boiling model, has made it the primary candidate for mechanistic modeling ventures. Mechanistic modeling of D is mostly carried out through the solving of force balance equations on the bubble. The forces incorporated in these equations are formulated as functions of the radius of the bubble and have been developed for, and applied to, only low-pressure conditions. On the other hand, for high-pressure conditions, no mechanistic information is available regarding the growth rates of the bubbles and the forces acting on them. In this paper, we use a Direct Numerical Simulation (DNS) coupled with an interface tracking method to simulate bubble growth under high (up to 45 bar) pressure, to obtain the kind of mechanistic information required for an RPI-type approach, thus up-scaling DNS to large scale simulation based on a two-fluid approach. In this paper we will be comparing the resulting bubble growth rate curves with predictions made with existing experimental data.

1. INTRODUCTION

Understanding, and having an ability to predict the disposition and intensity of nucleate boiling, is plainly of great importance in water-cooled nuclear reactor design and safety analysis. Void distribution influences "nuclear" matters such as neutron moderation, can affect chemistry and crud deposition, and has obvious heat transfer and surface temperature significance. The incorporation of a reasonable representation of nucleate boiling into general-purpose CFD codes used for nuclear core modeling is a current major development area for authors of such codes.

Such component-scale modeling of nucleate boiling is generally performed via a heat flux partitioning approach. In essence, this provides a closure relation between wall temperature and near-wall fluid temperature. The wall heat flux is considered to be able to be represented by three components, namely ordinary single-phase convection, evaporation, and "quenching"; the flow of relatively cool liquid towards the wall as it re-fills the volume previously occupied by a departing bubble. The semi-empirical representations of these components rely primarily upon experimental observations to estimate the main parameters involved; the bubble departure frequency, the bubble departure diameter, the nucleation site density, and the 'normal' convective cooling of the surface between the bubbles.

Increasingly sophisticated interface tracking CFD codes, incorporating interface mass transfer, are becoming able to generate quite high fidelity predictions of these complex events. This makes the use of such codes a possible complement to reliance on experimental observation to obtain the empirical relations needed for the component-scale modeling.

For obvious reasons, observations of boiling at high pressures tend to be much more limited than those at low pressures. Amongst other things, this forces much reliance in high-pressure component scale boiling modeling on extrapolations of data obtained at much lower pressures. Augmentation of pressure information, by the conducting of reliable high-pressure simulations, is thus a very desirable objective. As part of this, of course, it is important to be confident that the simulations themselves are indeed reliable.

We are fortunate that a set of high-pressure boiling measurements have been recently reported by Sakashita [1]. There have not yet to our knowledge been any published attempts at simulating these. In this paper, we attempt such a simulation, which is also the first publication of an attempt to simulate high pressure boiling using the PSI-BOIL code. Our particular focus will be an attempt to predict correctly the bubble growth rate, which is fundamental to most of the phenomena at issue.

In Section 2 we discuss the extant experimental evidence on bubble growth rates, and discuss earlier, largely analytical, attempts at predicting such growth. In Section 3 we provide a very brief summary of the modeling embodied within the PSI-BOIL code. The experiment of Sakashita is outlined in Section 4, and the computed results are compared with it. Finally conclusions are drawn in Section 5.

2. BUBBLE GROWTH RATE FORMULATIONS

There have been a considerable number of experiments aimed at measuring bubble growth rates, both within the bulk of a superheated liquid, and in a thin superheated layer adjacent to a surface.

Most were performed at constant wall heat flux conditions ([2] [3]). Lee et al. performed experiments with constant wall temperature and studied pool boiling of R11 and R113 for saturated boiling conditions [4].

Semi-empirical fitting of observed growth rates in these experiments generates a remarkably consistent form, with in addition quite uniform numerical scaling factors. The general form of the expression found is

$$R_P = A N_{Ja} \sqrt{\alpha_l t} \quad . \tag{1}$$

Various publications proposed differing values for the constant A, of [5] : $(12/\pi)^{0.5}$; [6] : $\pi^{0.5}$; [3] : $2/(\pi)^{0.5}$ (N_{Ja} < 100) (i.e. constant values of 1.95, 1.77, 1.13). These experiments were very largely performed at atmospheric pressure.

At higher pressures the physical properties of water are quite different. Volume ratios for liquid and vapour can be two orders of magnitude lower, surface tension can be ~an order of magnitude lower, 'contact' conditions between the heated surface and the liquid-vapour interface can be very different, as can the heat transfer through the micro-layer if at all one exists. The net result of all this is that the bubble growth rate is expected to be lower and the detachment radius much smaller.

Labunstov et al. analyzed bubble growth rates for water at high pressures (up to 10 MPa) and reported a bubble growth rate given by the following correlation [7]:

$$R_p = \sqrt{2\beta \cdot N_{Ja} \cdot \alpha_l t} \tag{2}$$

where β is a numerical coefficient which includes the effect of the contact angle and the thickness of the conduction layer near the bubble base. Akiyama et al. carried out an experiment for water boiling on a horizontal 8-mm-diameter cylinder at pressures of 0.1 to 1.5 MPa [8]. They reported that the bubble growth rate becomes lower with increasing pressure, and that it could be expressed approximately by

$$R_p = fn(t^{0.2}) \tag{3}$$

at 1.5 MPa. This relation is quite different from Eqns. (1) and (2).

However both these studies did not use any high-resolution visualization techniques for their study and hence only very rudimentary understanding of the underlying phenomenon is available.

3. NUMERICAL METHOD

3.1 General Characteristics

PSI-BOIL is a DNS code in which a single set of Navier-Stokes equations is solved based on a staggered finite-volume algorithm on Cartesian grids using an interface tracking method together with a mass-conserving phase change model. It has been developed at PSI over several years, and is, as the name implies, focused on the simulation of boiling process. Further details of the code in general, and of the particular aspects outlined below that are of most relevance to the present study, are given in the references cited [9][10].

3.2 Interface Tracking

The colour function is introduced as a volume fraction of liquid in a cell. The governing equation for the colour function is:

$$\frac{\partial \phi}{\partial t} + \nabla.(\phi \vec{u}) = -\dot{m}\frac{1}{\rho_l} \tag{4}$$

where $\dot{m}$ is the mass transfer rate in kg/m^{3}s computed in the phase change model. Here $\dot{m}$ is positive for vaporization, and negative for condensation. The derivation of Eq. (4) is given in Appendix A in [2]. The advection term is computed with the CIP-CSL2 method, which features high accuracy both in mass conservation and interface shape. To avoid the smearing of the colour function, a sharpening equation is employed:

$$\frac{\partial \phi}{\partial \tau} + \nabla.(\phi(1-\phi)\vec{n}) = \nabla.(\varepsilon\nabla\phi). \tag{5}$$

3.3 Surface Tension Model

In two-phase flows, the modeling of the surface tension is an important factor. In PSI-Boil this is done using the 'Continuum Surface Force' (CSF) model developed by Brackbill [11] to represent the surface-tension and wall- adhesion forces. In this paper this will referred to as the 'original' CSF model. There is a new, modified version of the CSF model that has been implemented based on the method proposed by Yokoi [12]

In the modified CSF model, curvature κ is firstly computed at cell center

$$\kappa = -\left(\nabla \cdot \vec{n}\right) \tag{6}$$

where $\vec{n}$ is the unit normal vector to the liquid-vapor interface and defined at cell center. Next, the curvature at the interface is computed using a linear interpolation. Then the curvature at the interface is extrapolated to cells around the interface. Consequently, the curvature used for the body force $\sigma\kappa\nabla\phi$ is based on the value at the interface.

The energy conservation equation can be written as:

$$C_p\left(\frac{\partial T}{\partial t} + \vec{u}.\nabla T\right) = \nabla.(\lambda\nabla T) + Q \tag{7}$$

The fundamental physical approximation / assumption made is that the liquid - vapour interface temperature is at the saturation temperature of the liquid. The normal gradient of temperature in the liquid at the interface is computed to evaluate the heat flux contributed to mass transfer. The conjugate heat transfer between solid and fluid flow is taken into account by using an immersed boundary method [13].

3.4 Micro-layer Model

A micro-layer model is considered essential for CFD simulation of a bubble growing at the wall. This model is required to resolve the thin liquid film that exists underneath growing bubbles. In the micro-layer model [10], which is also used in this paper, the liquid micro-layer thickness is a variable, and the

thickness decreases and finally reaches a dry condition due to the vaporization. The heat flux in the micro region is directly computed from the micro-layer thickness, wall temperature and the liquid-vapor interface temperature. The initial thickness of the micro-layer, δ_0, is given by the equation proposed by Utaka *et al.* [14]:

$$\delta_0 = C_{slope} r_L$$

(8)

where r_L is the horizontal distance from a nucleation site to a certain point underneath a growing bubble, C_{slope} is a constant obtained from measurement. For instance, $C_{slope} = 4.46 \times 10^{-3}$ for water and $C_{slope} = 1.02 \times 10^{-2}$ for ethanol boiling from a heated quartz glass surface at atmospheric pressure. It should be emphasized that C_{slope} is the only empirical parameter for this model, and is much more straightforward than other existing micro-region models [15, 16], in which several unknown parameters – such as the dispersion constant, the adsorbed film thickness, the gradient of the micro-layer film thickness at the extremities of micro-region – all need be assigned appropriate values. Hereafter, we refer C_{slope} measured for water by Utaka et al. as $C_{Utaka} = 4.46 \times 10^{-3}$.

4. RESULTS AND DISCUSSION

4.1. Sakashita's High Pressure Boiling Experiment

The objective of Sakashita's experiment was to make detailed observations of the boiling behavior on horizontal and vertical surfaces during saturated pool boiling of water at pressures from 0.35 to 5 MPa. The high pressure set-up was a cylindrical cell with an inner diameter of 50 mm and a height of 150 mm. Sapphire windows were installed to enable the boiling phenomena to be observed. This was done using a high-speed video camera and a microscope, with the video images analyzed manually. The measurements were predominantly of the nucleation site densities and the growth rates of the primary bubbles. For this current study, we will focus only on the horizontal surface experiments that were performed. The heating surface was a nickel foil, 8microns thick, 3–4 mm wide, and 27.5 mm long. The heat-transfer surface was heated with a DC power supply and the temperature of the heating surface was estimated from the change in the electric resistance of the nickel foil. A general view of the set-up and results can be seen in [1] .

4.2. Conditions of Simulation:

The computational domain is a cuboid of dimension 0.150 mm $\times$ 0.150 mm $\times$ 0.158 mm, including nickel heater of 8 μm thick at the bottom. All cases of the simulation were conducted for saturated pool boiling conditions. The working fluid is water and steam at a system pressure of 44.7 (bar). The material properties of the working fluid and the condition of the heated wall are listed in Table 1.

The simulation only attempts to simulate the bubble growth from a seed bubble existing on the wall and does not attempt to model the nucleation process itself. Consequently, it is expected that the thermal boundary layer near the wall has already developed at t = 0 s. The thickness of this thermal boundary layer is assumed to be similar to the natural convection thermal boundary layer thickness and is estimated based on the assumption that the wall is superheated at t=0 s and the far-off bulk liquid is at saturation temperature. The temperature of the fluid in the domain was set to vary linearly from the superheat temperature near the wall to the saturation temperature of the far-off fluid over a distance corresponding

to the thickness. At t = 0s, the entire solid is assumed to be uniformly at the superheated temperature The initial size of the seed bubble was specified to be of one grid cell width and its shape is hemispherical. The simulations were carried out with the coarse grid of 262,144 cells (Table 2). All the simulations in this paper is focused on the growth and departure of the first bubble.

Table 1 Fluid and Solid Surface Properties.

Fluid Properties at 44.7 bar	Water	Steam
Dynamic Viscosity (Pa.s)	1.03e-4	1.78e-5
Density (kg/m^3)	788.25	22.539
Specific Heat (J/kgK)	4949.3	4214.5
Thermal Conductivity (W/m.K)	0.61293	0.053181
Surface tension coefficient (N/m)	0.024	
Expansion ratio (kg/m^{3}K)	-1.6	-0.101
Solid Properties: Nickel		
Density (kg/m^3)	8908.0	
Specific Heat (J/kgK)	444.0	
Thermal Conductivity (W/m.K)	90.9	

Table 2 Computational Grid

Mesh	Grid A (Coarse)	Grid B (Medium)	Grid C (Fine)
Minimum Cell size (m)	2.00×10^{-6}	1.33×10^{-6}	1.00×10^{-6}
Number of Cells	262,144	884,736	2,097,152
Computational domain: $(1.50 \times 10^{-4}) \times (1.50 \times 10^{-4}) \times (1.58 \times 10^{-4})$ m^3			

4.3. Parasitic Currents

Figure 1 is representative of the temperature contours obtained during the growth cycle of the bubble; The temperature contour indicates that the fluid temperature on either side of the interface, that is in contact with the superheated liquid layer (macro-interface of the bubble), is lower than the rest of the fluid; and it can be concluded that this is due to the phase change occurring at this interface. As the interface temperature is assumed to be a constant (= saturation temperature) in PSI-BOIL, the heat flux (and consequently phase change) across the macro-interface is the cause of this temperature drop. The temperature contours also indicate that on the liquid side of the macro-interface, non-uniformity in the temperature contours can be seen. The velocity vectors at these locations indicate increased circulation and vortex-like structures. These are known as parasitic currents, a by-product of the original CSF model used in these simulations, and are purely a numerical artifact. The parasitic currents are as a result of a considerably large curvature (i.e. small bubble size of the order of 10 μm) and they seem to cause an increased heat transfer at the interface. In order to reduce the occurrence of these unphysical currents the modified CSF model was implemented.
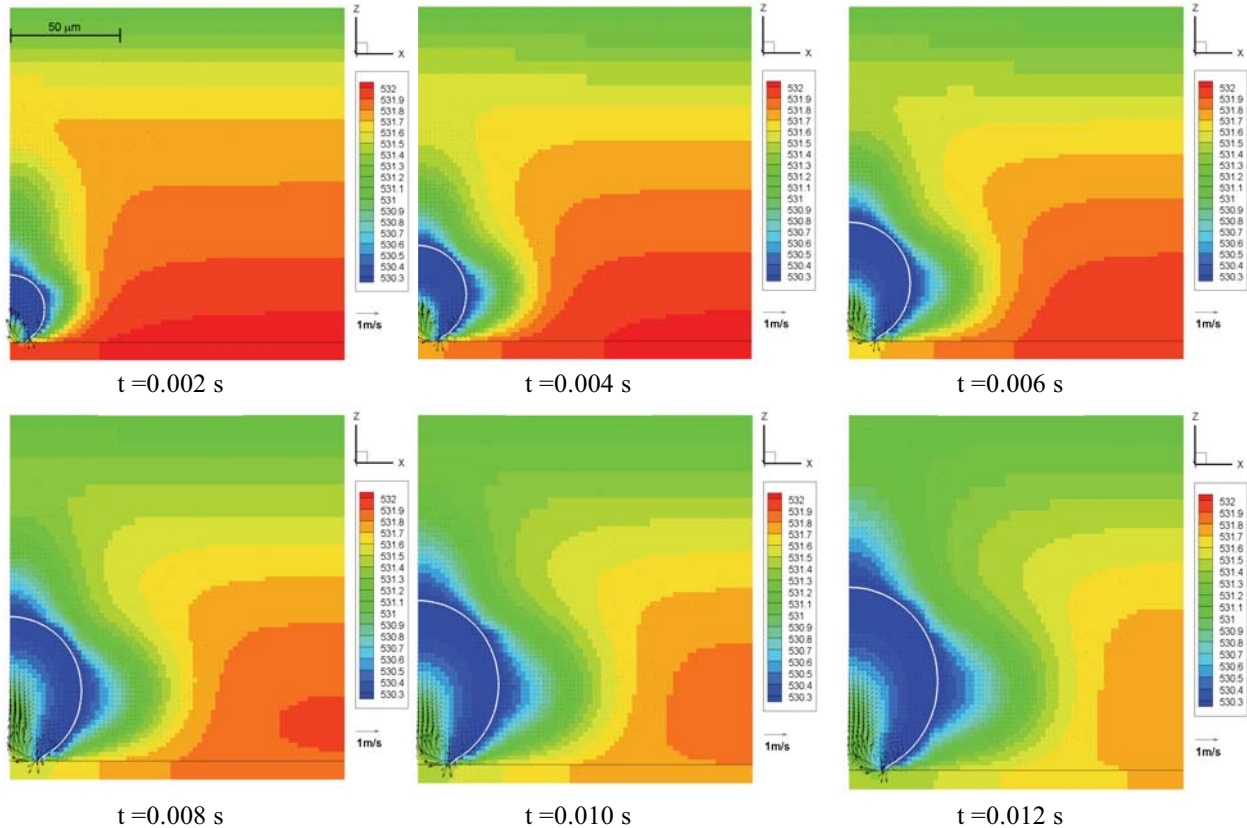
Figure 1 Parasitic currents: Temperature contours and velocity vectors with original CSF model. Images are from *t* = 0.002 s to 0.012 s at every 0.002 s.

Figure 2 shows the temperature and velocity vectors of the bubble growth and it can be seen that the unphysical parasitic currents are significantly reduced. By comparing the temperature contours and velocity vectors of the original and modified CSF model simulations, some important effects of the presence of parasitic currents can be observed- (a) The parasitic currents at the triple contact line cause a vapour plume to rise into the bubble; the velocity vectors indicate that the velocity magnitude of the vapor plume rising from the wall is high (b) the presence of parasitic currents result in cooler heater temperatures. Though presence of parasitic currents appear to modify the temperature and velocity contours, the bubble growth rate predicted by both the original CSF and modified CSF model is similar to that observed in the experiment (Figure 3). For both cases PSI-BOIL seems to achieve a very good prediction of the bubble growth rate at 44.7 bar

4.4. Effect of Micro-layer

As mentioned earlier PSI-BOIL was able to predict the growth rate of the bubble at the high pressure of 44.7 bar very well; however, it could not predict the time of detachment of the bubble accurately. A likely cause for this prolonged attachment of the bubble to the wall could be the micro-layer model. The micro-layer model implemented in PSI-BOIL is a model that was developed from experiments conducted at atmospheric conditions. For high pressures, no micro-layer experiments have been performed and hence we do not know if the micro-layer exists at all at elevated pressures. Labunstov et al. observed the bubble behavior at high pressure and theorized that the bubble growth is primarily governed by the evaporation

of liquid close to the bubble base [7]. They postulated that as the excess enthalpy of the superheated bulk liquid surrounding the bubble is small at high pressures the superheated layer would not contribute much to the evaporation. In this paper, we investigate this issue using CFD simulations. We also try to analyse if the thickness of the micro-layer is a likely cause for the delay in the bubble departure.
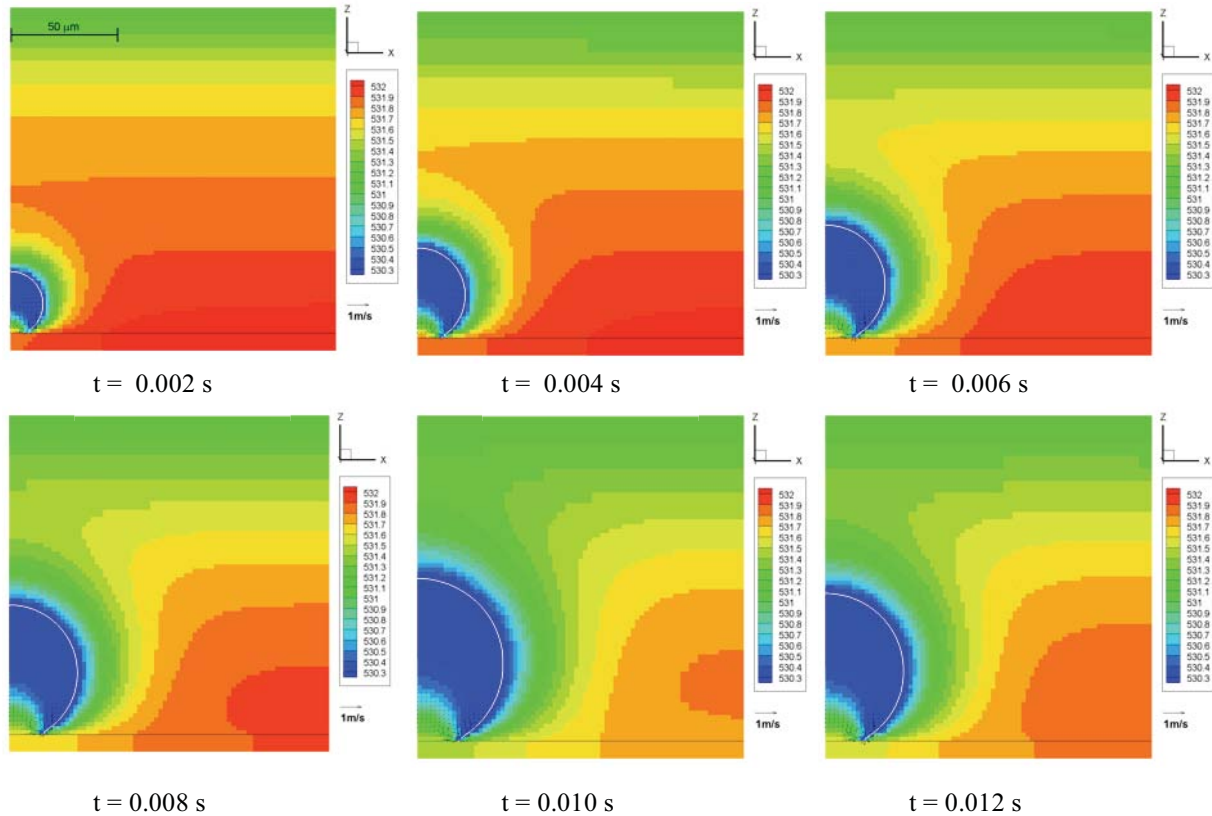

Figure 2 Reduced parasitic currents: Temperature contours and velocity vectors with modified CSF model. Images are from _t_ = 0.002 s to 0.012 s at every 0.002 s.
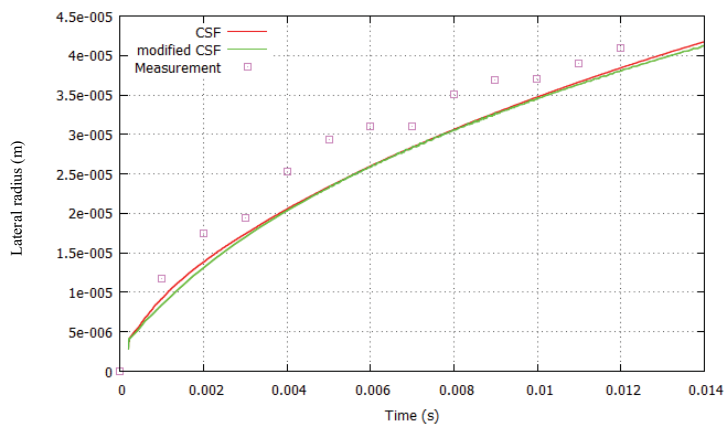

Figure 3 Bubble growth rate predicted for 44.7 bar Sakashita test case[1].

Consequently, simulations are performed wherein (a) the size of the micro-layer slope is reduced to 10 % of it's atmospheric value (b) the micro-layer model is completely removed, and the results are analysed.
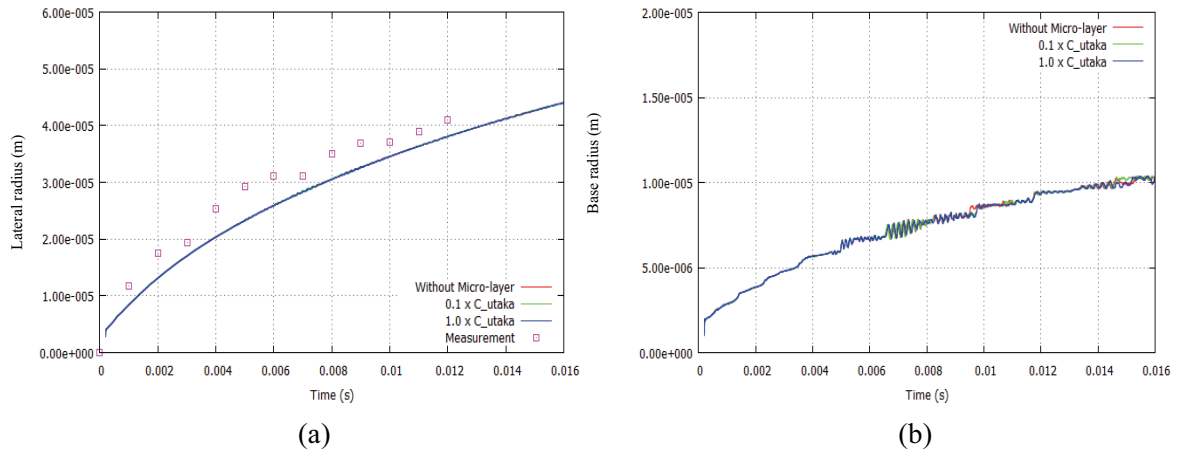

(a)

(b)

Figure 4 Effect of micro-layer thickness on (a) lateral radius and (b) base radius.

$t = 0.002$

$t = 0.004$

$t = 0.006$
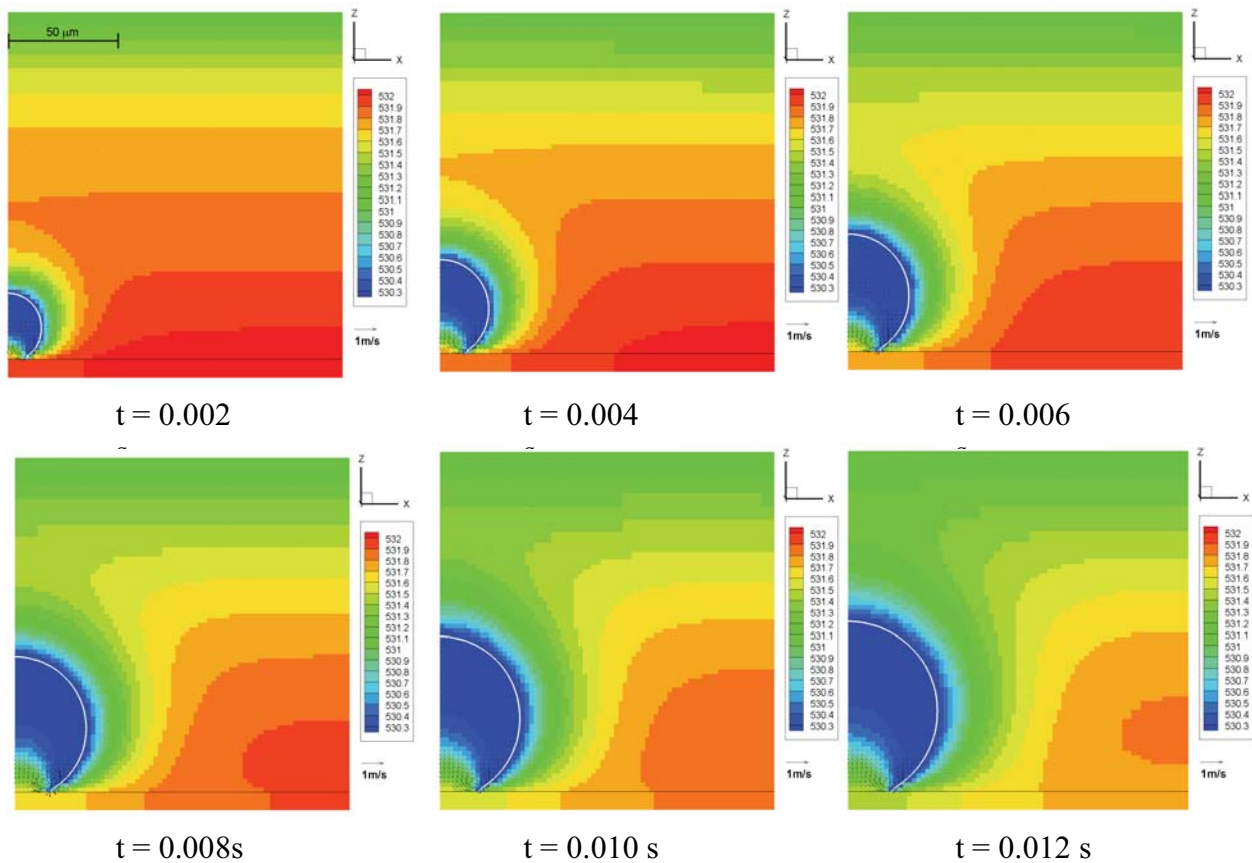
$t = 0.008$s

$t = 0.010$ s

$t = 0.012$ s

Figure 5 No microlayer: Temperature contours and velocity vectors with modified CSF model. Images are from $t = 0.002$ s to 0.012 s at every 0.002 s.

The predicted bubble growth rate (Figure 4), as well as the temperature and velocity plots do not vary much for the original and reduced micro-layer thickness. The time evolution of the temperature distribution with no micro-layer (Figure 5) is almost identical to the one with micro-layer (Figure 2). This indicates that the presence of a micro-layer model has little influence on bubble growth under the corresponding condition (i.e. water at 45 bar). This is further supported by the fact that the rate of growth of the base radius of the bubble does not change with the presence of the micro-layer (Figure 4b). This could imply that the majority of the phase change is occurring from the macro interface of the bubble and only a negligible amount occurs from the micro-layer region. In looking at the phase change rate for the no micro-layer case (Figure 6) it can clearly be seen that a large magnitude of the phase change occurs near the triple contact line but at the macro-interface level and not in the micro-layer.
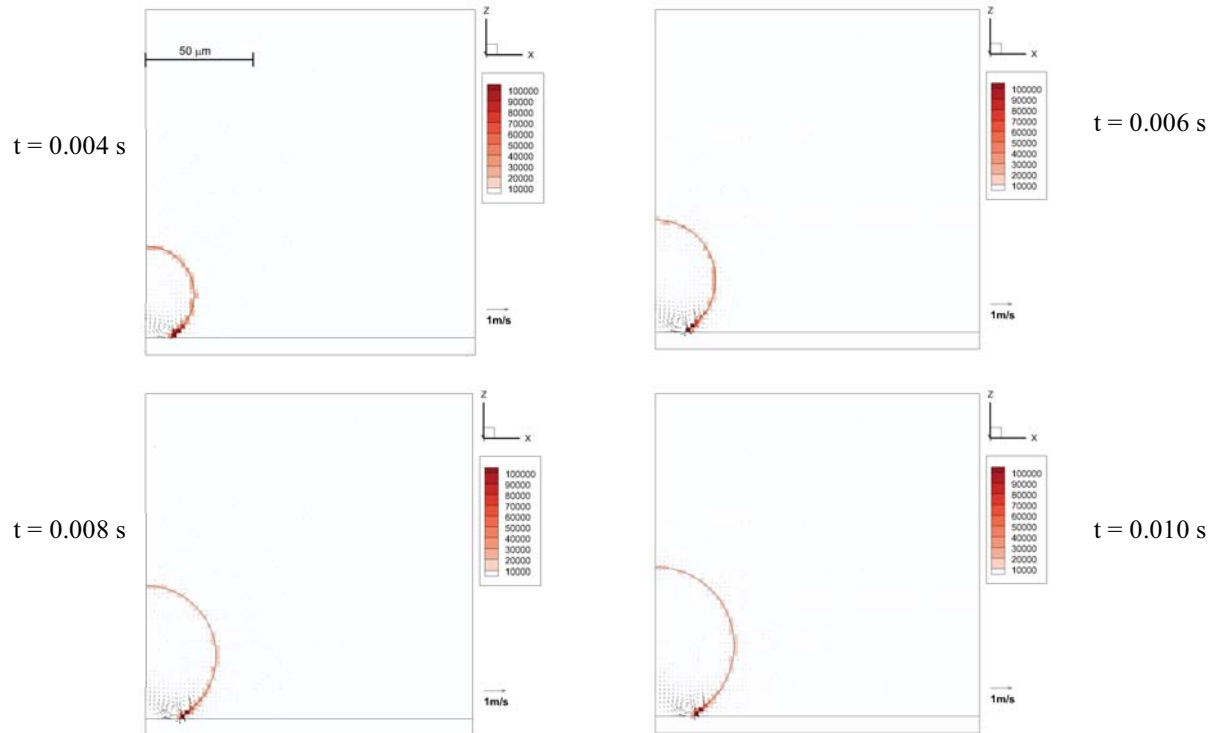

Figure 6 No micro-layer: Phase change rate distribution in kg/sm^3 from t = 0.004 s to 0.01 s at every 0.002 s.

4.5. Grid Dependency Test

In the PSI-BOIL code, the mass transfer rate is directly computed from the heat flux coming to the liquid-vapor interface from the surrounding fluid or solid. The heat flux is based on the temperature gradient, which is influenced by grid spacing, if sufficiently small grid is not used. Thus a grid dependency test is required. In addition, the seed bubble is initially hemi-spherical in shape, the radius being typically one cell width of the underlying grid. This means that the model is dependent on the discretization (grid spacing), and a grid refinement study is then required; three grid levels are used to test the same. The number of cells for each grid is listed in Table 2. As bubble growth rate was found to be independent of the micro-layer model, the dependency test was performed without the micro-layer model. Figure 7 shows the variation in the lateral and base radius of the growing bubble for the each grid level. The growth rate of the lateral radius increases with decreasing of grid size. This tendency is considered to be reasonable, because smaller grid can evaluate steep temperature gradient more accurately (i.e. the coarser grid underestimates temperature gradient). Such a condition is observed around the liquid adjacent to the liquid-vapor interface. The base radius does not seem to vary greatly with grid size, indicating that the

wall adhesion force implemented and defined in the CSF model is more independent from the grid spacing. Figure 8 shows the difference in the temperature contours and velocity vectors for the different grid sizes.
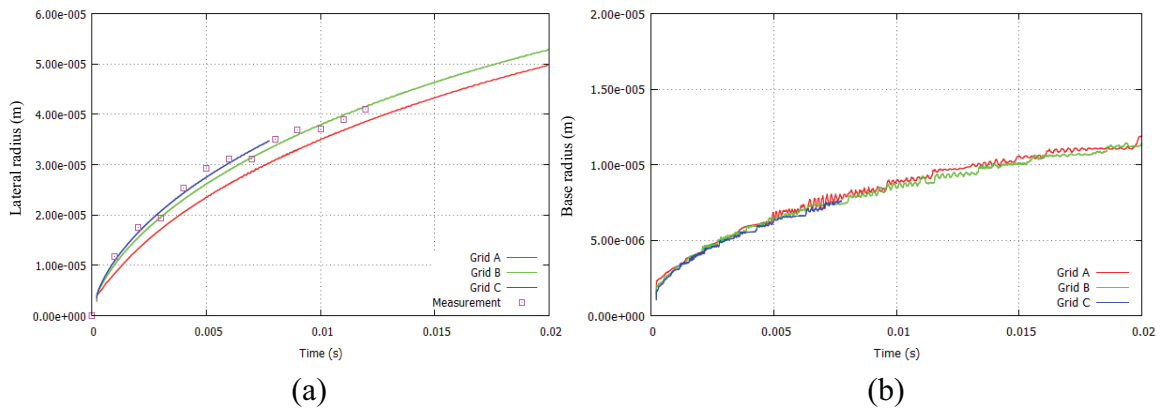

(a)   (b)

Figure 7: Grid dependency test for (a) lateral radius and (b) base radius.
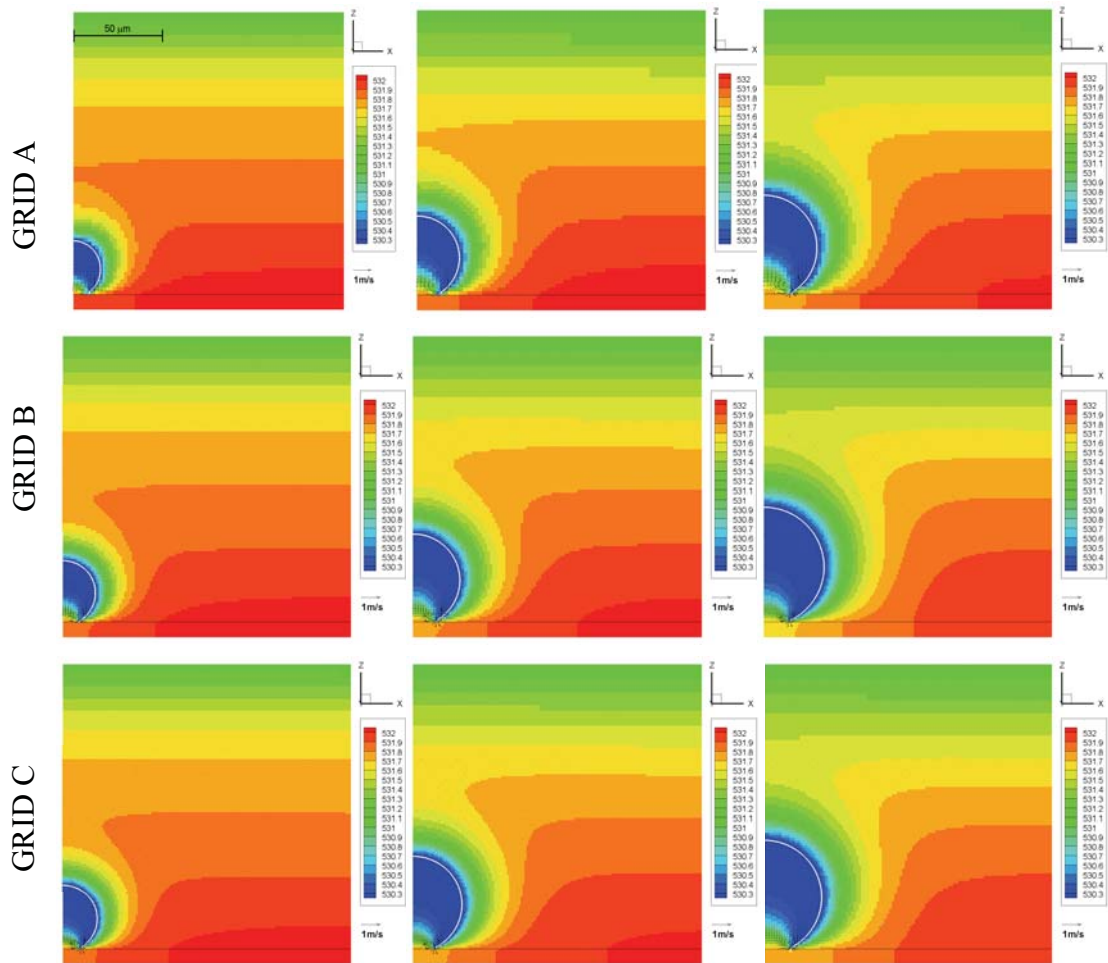

Figure 8: Grid dependency study: Temperature contours and velocity vectors. Images are from
$t = 0.002$ s to 0.006 s at every 0.002 s.

5. CONCLUSIONS

1. The bubble growth rate predicted by PSI-BOIL agrees well with that of the 44.7 bar pool boiling experiment of Sakashita [1]. This indicates that PSI-BOIL can predict bubble growth rates at higher pressures and can be used to obtain the bubble growth rate expression for use in component scale boiling modeling. This is indeed the thrust of the work that is currently underway wherein, a growth rate equation applicable for different pressures is being developed.

   For the current case, the bubble growth rate predicted by PSI-BOIL matches the experimental observations of Sakashita [1]; consequently the correlation that was proposed in [1] i.e.

$$R_p = C\sqrt{\alpha_l t} \tag{9}$$

   where $C = \sqrt{2\beta N_{Ja}}$ and $\beta = 3$, can be used for the component-scale bubble departure diameter modeling at 45 bar in place of the commonly used Plesset and Zwick equation (which is applicable for atmospheric pressures). It is important to note that the growth rate at 45 bar varies as a $\sqrt{N_{Ja}}$ and not N_{Ja} (atmospheric pressures).

2. Unphysical temperature distribution is observed for the case using the original CSF model due to strong intensity of parasitic currents. The parasitic currents result from considerably large curvature (i.e. small bubble size of the order of 10 μm) in the corresponding simulation case. The unphysical temperature distribution is reduced considerably, once the modified CSF model is used

3. The presence of the micro-layer model implemented in the PSI-BOIL code as well as its thickness has little influence on bubble growth for saturated pool boiling of water at 45 bar with respect to the bubble lateral diameter. It is observed from the simulations that maximum phase change is observed near the triple contact line region but at the macro scale level.

6. NOMENCLATURE

Variables	Meaning	Unit
A	constant	-
C_p	volumetric specific heat	J/ m^{3}K
g	gravitational acceleration	m/s^2
N_{Ja}	Jakob number	-
p	pressure	N/m^2
Q	heat source	W/m^3
R_p	bubble radius	m
T	temperature	K
t	time	s
u	velocity	m/s

Greek

α	thermal diffusivity	m^2/s
ε	coefficient for interface thickness	m
ϕ	colour Function	-
λ	thermal conductivity	W/mK
ρ	density	kg/m^3
τ	pseudo-time	-

Subscripts

l	liquid

7. REFERENCES

1. H. Sakashita, "Bubble Growth Rates and Nucleation Site Densities in Saturated Pool Boiling of Water at High Pressures," *J. Nuclear Sci. Tech.,* 48, pp. 734-743 (2011).
2. C.H. Han, P. Griffith, "The mechanism of heat transfer in nucleate pool boiling- Part I Bubble initiation, growth and departure," *Int. J. Heat Mass Transfer*, 8, pp. 887-904 (1965).
3. R. Cole, H. L. Shulman, ''Bubble growth rate at high Jakob numbers,'' *Int. J. Heat Mass Transfer*, 9, pp. 1377-1390 (1966).
4. H. C. Lee, B. D. Oh, S. W. Bae, M. H. Kim, "Single bubble growth in saturated pool boiling on a constant wall temperature surface," *Int. J. Multiphase Flow*, 29, pp. 1857-1874 (2003).
5. M.S. Plesset, S.A. Zwick, "The growth of vapor bubbles in superheated fluids," *J. Appl. Phys.,* 25, pp. 493-500 (1954).
6. H. K. Forster, N. Zuber, "Growth of a vapor bubble in a superheated liquid," *J. Appl. Phys.*, 25, pp. 474-478 (1954).
7. D. A. Labuntsov, B. A. Kol'chugin, V. S. Golovin, É. A. Zakharova, L. N. Vladimirova, "Study of the growth of bubbles during boiling of saturated water within a wide range of pressures by means of high-speed moving pictures," UCS 536.423 1, 404–409 (1964), [translated from Teplofizika Vysokikh Temperatur, 2, pp. 446-453 (1964)].
8. M. Akiyama, H. Tachibana, N. Ogawa, "Effects of system pressure on bubble growth rate," *Trans. JSME*, 35, pp.117-126 (1969), [in Japanese].
9. Y. Sato, B. Niceno, "A sharp-interface phase change model for a mass-conservative interface tracking method", *J. Comp. Phy.*, 249, pp. 127-161 (2013).
10. Y. Sato, B. Niceno, "A new concept of micro-region model: A depletable micro-layer for nucleate pool boiling flows," *2nd Int. Conf. Numer. Meth. Multiphase Flows* (ICNMMF-II), Darmstadt, Germany, pp. 202-203 (2014).
11. J.U. Brackbill,, D.B. Kothe, and C. Zemach, "A continuum method for modeling surface tension," *J. Comp. Phy.*, 100, pp. 335-354 (1992).
12. K. Yokoi, "A practical numerical framework for free surface flows based on CLSVOF method, multi-moment methods and density-scaled CSF model: Numerical simulations of droplet splashing," *J. Comp. Phy.*, 232, pp. 252-271 (2013).
13. B. Ničeno, F. Reiterer, A. Ylönen, H.M. Prasser, "Simulation of single-phase mixing in fuel rod bundles, using an immersed boundary method", *Physica Scripta*, 88 (2013).
14. Y. Utaka, Y. Kashiwabara, M. Ozaki, "Microlayer structure in nucleate boiling of water and ethanol at atmospheric pressure," *Int. J. Heat and Mass Trans.*, 57 pp. 222-230 (2013).
15. P.C. Stephan, C.A. Busse, "Analysis of the heat transfer coefficient of grooved heat pipe evaporator walls," *Int. J. Heat and Mass Trans.*, 35, pp. 383-391 (1992).
16. J.H. Lay, V.K. Dhir, "Shape of a vapor stem during nucleate boiling of saturated liquids", *J. Heat Trans.*, 117, pp. 394-401 (1995).